

Planar probe array for bidimensional mapping of the ion flux profile of a miniaturized ion thruster

IEPC-2019-777

*Presented at the 36th International Electric Propulsion Conference
University of Vienna • Vienna, Austria
September 15-20, 2019*

Lui Habl¹, Dmytro Rafalskyi², Elena Zorzoli Rossi³ and Ane Aanesland⁴
ThrustMe, Verrières-le-Buisson, 91370, France

Abstract: The characterization of the plume profile of low-power ion thrusters is imperative for the evaluation of the impacts in performance caused by the miniaturization process. Here we present the development of an instrument, consisting of an automatized array of planar probes, capable of performing two-dimensional mappings of the ion current density profile produced by the thrusters. In order to validate the instrument, we conducted experiments using a low power gridded ion thruster NPT-30. The collected data and proposed procedure to extract both information about total ion current and divergence half-angle of the two-dimensional maps are also presented. The results of the experiments show a close agreement between the ion current measured and the expected values for the operational regimes of the thruster. It is also shown that the divergence half-angle has a decreasing profile with perveance within the range studied here, showing that the thruster is operating under sub-optimal regime over the chosen operational points.

Nomenclature

A_0	= area of central probe, m ²	T_e	= electron temperature, eV
A_{eff}	= effective probe area, m ²	V_p	= probe bias voltage, V
A_i	= estimated probe area, m ²	α	= divergence half-angle, rad
a, b	= parameters of Sheridan's model	η	= parameter of Sheridan's model
D	= diameter of the probe, m ²	λ	= great-circle central angle, rad
I_b	= total ion current, A	λ_D	= Debye length, m ²
$I_{b,a}$	= axial ion current, A	ρ_p	= parameter of Sheridan's model
J_i	= ion current density, A/m ²	ϕ_0	= position of central probe, rad
N_p	= total number of probes	ϕ_i	= estimated probe position, rad
R	= radius of the instrument arc, m	ϕ_f	= position of final probe, rad

I. Introduction

With the rise in complexity of small satellite missions (< 180 kg), low-power electric propulsion (EP) systems have been increasingly employed to perform tasks not commonly considered before in this context, such as precise orbit positioning, maneuvering, drag compensation, and spacecraft decommissioning [1]. Between the many concepts of miniaturized thrusters available, the gridded ion thruster (GIT) is often chosen for its scalability, relative high efficiency levels, and versatile propellant utilization [2]. Nevertheless, the miniaturization process of GITs tends to compromise their performance considerably [3], therefore the measurement of the plume characteristics is imperative for the investigation of loss mechanisms related to lifetime and efficiency.

In the last decades, numerous types of diagnostic methods [4] were proposed and extensively studied for the characterization of a thruster's plume, permitting precise acquisition of different parameters as current density,

¹ PhD candidate, ThrustMe/LPP/École Polytechnique, lui.habl@thrustme.fr

² Chief technology officer

³ Experimental engineer

⁴ Chief executive officer

energy distribution, molecular composition, amongst others. Particularly, for the measurement of the ion current density profile, which is one of the most important parameters to measure in order to evaluate the performance of a thruster, Faraday probes in one of its many varieties has been one of the most successful methods so far [5]. This type of measurement consists in using an electrostatic probe with a considerably large area to collect and measure the impinging ion saturation current while repelling electrons usually by the application of a bias voltage. Despite its simplicity, this concept can give rise to undesired effects such as sheath expansion [6], collection of slow charge exchange ions [7], and emission of secondary electrons with impact of ions [8]. In order to mitigate these phenomena, several different techniques have been proposed in the literature [5] [7] [9].

Within the several different applications of Faraday probes in the propulsion context, one of the most common is the mapping of ion current density in the near and far field plume region, which permits the determination of the beam divergence half angle and total ion current being emitted by the thruster; two important factors to the determination of the system's performance. There are several examples available in literature showing methods to perform such scans; the most typical is using a probe placed on a moving arm that moves on an arc that passes through the centerline of the thruster [8]. Other methods are the usage of an automated system that can move a single sensor in a bidimensional plane [10] and an array of sensors placed over an arm that can scan the beam over a curved surface [11] [12]. We present in this article the development of a system like the last-mentioned type, consisting on an arc containing an array of naked Faraday probes (also called planar probes) designed for measurement, in two dimensions, of the beam profile generated by a low-power gridded ion thruster.

The instrument developed in this work has as its main goal to improve the automation of the qualification process of miniature ion thrusters produced at ThrustMe and aid the investigation of different physical effects while developing new systems. Specifically, this instrument is very important in the development of RF acceleration thrusters, because in this setting the beam current cannot be obtained from the current collected by the grids and need to be measured directly from the plume [13] [14] [15]. With the successful testing of the sensor array, final design and manufacture, the system will be adopted as a standard measurement device for comparison and acceptance of thrusters of the NPT-30 family on the production line at ThrustMe.

The first part of this paper presents the working principles and construction of the instrument. The design of the probe array was based on available plume models and resulted in a gaussian-like variation of position and area of the probe sensors, which aims is primarily to optimize ion current detection at each angular position. Furthermore, as planar probes have the tendency to overestimate the measured ion current density [5], we also present the methods employed to mitigate the errors caused by sheath expansion and electron secondary emissions, permitting the correction of the data through a semi-empirical model.

In the second part of the article we present the obtained experimental results. In the context of this work, the instrument was used to measure the ion current density profile of the NPT-30, a propulsion system based on an RF gridded ion thruster with beam diameter of about 3 cm [16]. The measurements were conducted at different operational regimes, described in the later sections. Finally, in the third part, we present a discussion about the capability of the system to characterize low-power ion beams and the quality of the data regarding the beam divergence and total ion current of the thruster at each operational mode.

II. Instrument design

A. Planar probes

In order to measure ion current density at each position, the instrument contains a set of 16 electrostatic planar probes which were biased to a given voltage to collect exclusively the ion saturation current in the beam. The probes are connected to an electrical circuit which consists of an array of measurement resistors and filtering capacitors that suppresses noise and bypass AC current component. On the other side of the signal lines, low pass filters ensure efficient noise suppression. The signal from the measurement resistors were acquired by a galvanically insulated data acquisition board which was biased together with the probe array to negative voltage for electron rejection. Figure 1 shows the simplified view on the measuring circuit block.

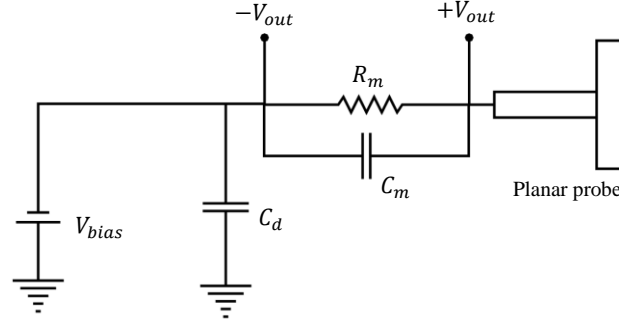


Figure 1 – Planar probe measurement circuit.

To balance the precision of the acquisition board through all channels, the systems was dimensioned so that all probes collected a similar current value and generated a similar voltage level for measurement. For this, the collection areas of the probes, the measurement resistors and the spacing between the probes were varied along the instrument arm. For this dimensioning procedure, we assumed the plume has an approximately gaussian distribution over the range of angles [17] in the form $J_i(\phi) \sim \exp -\beta\phi^2$. From that, it was possible to calculate the probes area and spacing values, in the form

$$\frac{A_i}{A_0} \approx \exp\left(2\frac{\phi_i^2}{\alpha^2}\right), \quad \frac{\phi_i}{\alpha} \approx \frac{1}{\sqrt{2}} \operatorname{erf}^{-1}\left(\frac{i}{a}\right) \quad (1)$$

Where A_i and ϕ_i are the areas and positions of the i -th probe from the center respectively, A_0 is the area of the central probe, α is the divergence angle of the assumed current distribution, $a = N_p \left(2 \operatorname{erf} \frac{\sqrt{2}\phi_f}{\alpha}\right)^{-1}$, N_p is the number of probes, and ϕ_f is the angular position of the last probe. From these expressions the approximate values for positions and probe sizes were calculated which served as basis for the mechanical design process described in the next section.

When using planar probes to measure current density in the plume, one of the most important concerns is the correction of the plasma sheath expansion in front of the probe when its bias voltage is decreased below the floating potential. This biasing increases the effective collection inducing an overestimation of the ion saturation current [8]. In order to mitigate this effect, we used the Sheridan's empirical model for the correction of the I-V curve *a posteriori* [18]. Sheridan developed this method from particle-in-cell simulations of the sheath formed in front of a double sided Langmuir probe, and was later experimentally verified by Lee and Hershkowitz [6]. Following the model, the expression for the effective area A_{eff} is given by

$$A_{\text{eff}} = A(1 + a\eta^b) \quad (2)$$

Where A is the physical area of the probe, $\eta = -V_p/T_e$, and V_p is the probe bias voltage. a and b are fitting parameters given by $a \approx 2.28\rho_p^{-0.749}$ and $b \approx 0.806\rho_p^{-0.0692}$, where $\rho_p = D/2\lambda_D$, D is the diameter of the probe and λ_D is the Debye length. Measurements with a Langmuir probe were conducted in order to determine the approximate parameters (plasma potential, V_p , and electron temperature, T_e) necessary for the corrections of the measured current.

B. Mechanical design

This instrument was conceived to be an inexpensive tool for the assessment of plume characteristics of miniaturized gridded ion thrusters NPT-30 in order to study the effects of modifications on the plume divergence and identify possible asymmetries. In this way, the design focused on the reduction of complexity and cost of the electrical and mechanical parts of the project.

The structure of the system consists on a stainless-steel arc with curvature radius of 269 mm, that holds the 16 planar probes. The arc is moved by two KH4238 stepper motors which have maximum static torque of 0.34 Nm and can rotate the structure 180 degrees from the bottom vertical position with a step length down to 0.10 degrees. In order to decrease the load on the motors, one aluminum counterweight was positioned on the end of each extremity of the arm. The motors were controlled externally by a driver circuit and a script able to synchronize the movement of the instrument and the acquisition system.

The planar probes were built in stainless-steel with four different diameters (4.1, 5, 6, 7, 25.46 mm) approximating the relation shown in the last section and were positioned along the structure using 0.5 mm thickness mica rings for insulation. The probes were connected through a set of silver coated wires to the internal circuit containing all the passive components necessary for measurement, which is positioned on the top of the right-hand side counterweight and is shielded to avoid interferences due to the background plasma. Figure 2 shows the details of the construction and its placement inside the vacuum system.

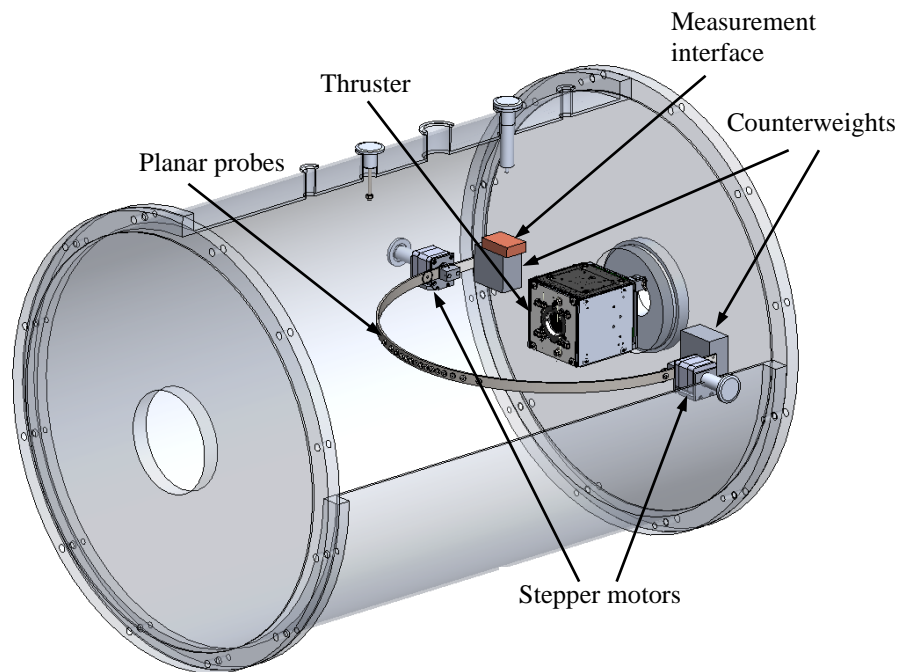


Figure 2 – Instrument construction and positioning inside the vacuum chamber.

III.Experimental setup

The first use for the new instrument was a series of experiments to scan the plasma plume of the NPT-30 propulsion system, which consists of a miniaturized RF gridded ion thruster using xenon as propellant. The thruster is the first French gridded ion thruster and is part of a 2U propulsion system, capable of proving between 2400 and 5000 Ns of total impulse, between 0.2 and 1.2 mN of thrust and consuming between approximately 25 and 60 W of power. The exhaust surface of the thruster has approximately 4 cm in diameter and, it uses a two-grid system for acceleration which, for the purpose of the present testing, uses a fixed acceleration voltage of 1 kV.

The aim of the experiment to scan the ion beam was to determine the characteristics of the plume of the thruster at a number of possible flight mode configurations. It is of interest to see how a slight change of some customizable parameters would modify the profile and the magnitude of the ion beam and affect the thruster performance. These changes can be performed remotely and allow the user to switch mode for different requirements at different points of the mission. The resulting changes in the plume have been documented for the main set of operational modes of NPT-30 at the moment of the present test campaign. The NPT-30 propulsion system operation is based on discrete modes, providing fixed performances at a given input power. The parameters that are used to obtain the different modes are: flow rate of a feeding gas, voltage of the screen grid and RF power. The corresponding power and thrust levels for the set of operational modes investigated in this work is given in Table 1.

The experimental arrangement is shown in Figure 2. All testing was conducted in ThrustMe's vacuum facility, which consists on a cylindrical vacuum chamber with 0.6 m in diameter and is 0.83 m long, and a pumping system equipped with a primary and a turbomolecular pump with total pumping speed of 2500 l/s (by N₂). During experiments, the backpressure was always maintained below $1.4 \cdot 10^{-5}$ mbar (Xe) and residual pressure was better than $5 \cdot 10^{-7}$ mbar. On the back flange of the chamber, the 1U thruster NPT-30 was installed. Thermal

management of the module was ensured by integrated thermal management system. Operation of the module was controlled by the internal power processing unit (PPU). Xenon storage and flow control system was replaced with the industrial grade mass flow controller connected to a xenon bottle at 70 Bar pressure. The module was powered with the 12 V DC voltage (range of accepted bus voltages is 10-30V), and communication with the module was performed using the CAN bus.

Inside the vacuum chamber, the measurement board of the instrument and the flange were connected via a multi-wire cable shielded with a copper braid to avoid electromagnetic interference over the measurement signals. In order to record the voltage from the signal wires, a 16-channel MCC USB-1608HS data acquisition board was used. This board is capable of simultaneous 16-bit acquisition at speeds up to 250 kS/s. The data was then transmitted to a Python script that was developed to control both the measurement board and the movement of the arm through an Arduino microcontroller board. All data was then stored and processed using dedicated algorithms.

At the beginning of the experiment the sensor arc was positioned below the thruster in a resting position (0°). Then, after the ignition procedure and establishment of the nominal thruster operation, the modes were set and, after a one-minute period to ensure steady-state, the instrument performed the scan of the plume with steps of 0.10 °/s up to 120 degrees (above the thruster). The control software ensures a synchronous operation between the thruster and the measurement system and allows the control in real time of the position and speed of the instrument.

Table 1 – Description of the investigated NPT-30 operational modes.

Mode	Total power (W)	Thrust (mN)
1	28.376	0.327
2	30.816	0.401
3	39.122	0.594
4	42.641	0.668
5	29.369	0.375
6	33.174	0.484
7	37.912	0.603
8	42.283	0.706
9	46.602	0.789
10	40.620	0.690
11	45.458	0.804
12	49.872	0.897
13	29.940	0.412
14	36.762	0.607
15	42.550	0.765
16	48.340	0.898
17	51.681	1.001
18	57.573	1.109
19	62.163	1.203

IV. Results and discussion

In order to evaluate the plume characteristics of the thruster and the performance of the instrument, 19 operational regimes were tested and underwent the measurement procedure; due to the large amount of data only a few key points have been selected to represent the behavior of the system. Each operational point produced a matrix with approximately 12800 data points from the 16 measured channels which permitted the reconstruction of a two-dimensional map of the current density distribution over the scanned spherical surface. Processing the maps permitted the calculation of performance metrics, such as the divergence angle and total ion current, and the evaluation of asymmetries.

During the experiments the reading of each channel, with the angular sweep of the instrument, produced an approximate bell-shaped curve resembling the behavior expected from other experiments present in literature [19]

[17]. Figure 3a shows the measured ion current density by 7 sensors during operation in mode 18 according to Table 1. In order to facilitate visualization, the measurement noise was reduced using a Savitzky–Golay filter. As can be seen, the channels respective to sensors at angular positions close to the thrust axis presented readings similar to the profile measured in single-probe experiments. The intensity of the curves decreased as the sensor angular distance from the center is increased.

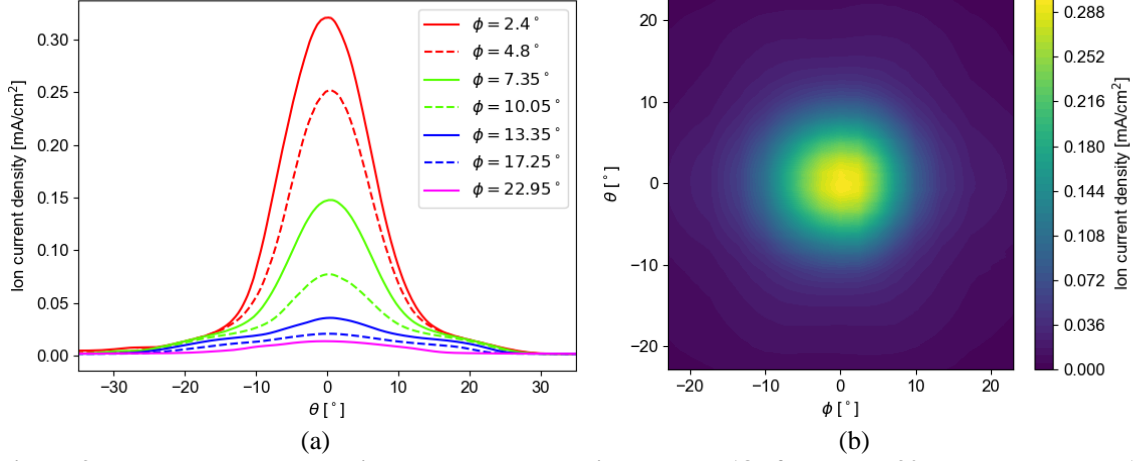


Figure 3 – Measurement by the instrument at operational mode 18 of the NPT-30, presented as the (a) signal measured by 8 channels of the array, (b) the reconstructed bidimensional map.

Each obtained data set consists of an approximately 800 by 16 points matrix having a much higher angular resolution in the direction of movement versus the azimuthal direction, causing the reconstruction of the bidimensional maps to necessarily have higher interpolation errors in the direction of the sensors. The resulting map of the operation of mode 18 is shown in figure 3b, a gaussian filter was applied to the data to ensure an improved visualization. In the plot it is possible to observe the central peak in ion current density as expected, with a continuous decrease in amplitude in outbound direction. It is also possible to observe a subtle hexagonal outline formed near the outer boundary of the domain, which can be associated with the hexagonal pattern of the grid holes in the NPT-30.

In order to calculate both total ion current and the divergence half-angle from the beam current maps it is necessary to perform the numerical integration of the data over a spherical surface. Brown et al. [8] describe the method commonly used in literature for a single-probe experiment, consisting on the integration of the current density in one dimension in half of the azimuthal domain. In the same work, they also show a method for the correction of the effect of a non-punctual origin of ions, taking in consideration the diameter of the plasma source. In the case of the present work it was necessary to do the integration in both directions of the density field, so the calculation of the total ion current over the domain is

$$I_b = R^2 \int_{-\frac{\pi}{2}}^{\frac{\pi}{2}} \int_0^{\pi} J_i(\theta, \phi) \sin(\phi) d\phi d\theta \quad (3)$$

where R is the radius of the instrument and $J_i(\theta, \phi)$ is the ion current density measured at a given position. To be employed, it was necessary first to re-center the data points on $(0, \pi/2)$ to ensure a correct correspondence to the standard spherical coordinates, the equation was then discretized and evaluated over the grid.

For the calculation of the divergence half-angle α it is necessary to determine the total axial current being emitted by the source. In the single-probe case this can be calculated by the decomposition of the current density in the direction of θ . On the other hand, in two dimensions this decomposition needs to be done using the central angle $\lambda(\theta, \phi)$ between the origin and the evaluated point, which consists on the angle determined by the “great-circle” distance between these two points. This angle can be derived from the haversine formula as being

$$\lambda(\theta, \phi) = 2 \sin^{-1} \left(\sqrt{\frac{1 - \sin \phi \cos^2 \theta}{2}} \right) \quad (4)$$

Noting that we can do the relation $\cos \lambda = \sin \phi \cos^2 \theta$ using equation 4, the expression for the axial ion current can then be written as

$$I_{b,a} = R^2 \int_{-\frac{\pi}{2}}^{\frac{\pi}{2}} \int_0^{\pi} J_i(\theta, \phi) \sin^2 \phi \cos^2 \theta d\phi d\theta \quad (5)$$

Integrating the data using the obtained formula, it is possible to calculate the divergence half angle as

$$\alpha = \cos^{-1} \left(\frac{I_{b,a}}{I_b} \right) \quad (6)$$

Using the described formulas, it was possible to calculate both parameters for the investigated operational modes. Figure 4 shows the plot of the total ion current versus the total power consumed at each mode. As can be observed, the total ion beam current grows linearly with the total thruster power, as it was expected. It is also observed that the values measured with the scanning arc hold a close relation to the values of the beam current measured directly on the grids.

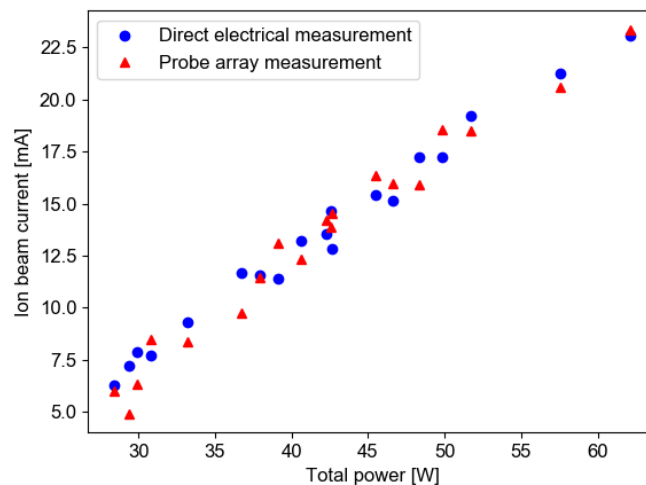


Figure 4 – Ion beam current over all studied operational modes, showing the comparison between the direct electrical measurements and the estimation from measurements performed by the probe array.

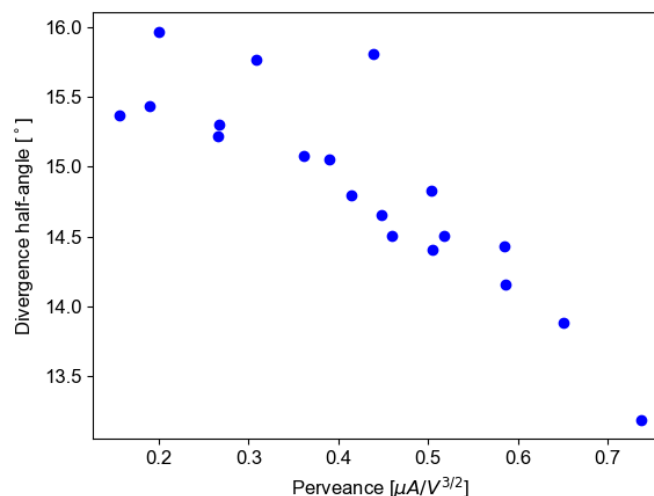


Figure 5 – Divergence half-angle dependence on perveance for all studied operational modes.

On figure 5, the plot shows the divergence half-angle calculated using the measured dataset. As can be observed, the divergence, for all operational modes, stay in the range between roughly 13 and 16 degrees, in agreement with other results obtained for gridded ion engines reported in literature [19]. Despite the slightly higher spreading in the current data set due to the non-linear dependence of both quantities, it is also possible to observe a decreasing divergence with the increase of perveance, meaning that the current set of grids of the NPT-30 has potential for higher thrust values comparing to the modes set used in the presented experiments (see Table 1).

As extensively studied in literature [19], the plasma meniscus topology near the grid holes reacts to the variation in the perveance in order to maintain the Child-Langmuir sheath near the acceleration orifice, effectively making the sheath more concave as the perveance decreases and more convex otherwise. This topology dictates how ions are accelerated through the channel, and on both extreme cases can lead to the complete defocusing of the beam. Thereby, to ensure the minimization of ion impingement on the acceleration grid and decrease the divergence level, it is necessary to approach the optimal value of perveance for this specific set of grids. Observing the measured divergence for a given set of operational modes of the NPT-30 engine, one can conclude that the thruster is currently working in an under-perveance regime, agreeing with the modeling results using the proprietary PIC (particle-in-cell) code. This indicates that in order to further optimize the ion focusing for this grid set it is necessary either to work under higher power levels or decrease the acceleration voltage applied, in case if lower beam divergency value is required for a specific mission.

V. Conclusion

In this work we presented the development process of a movable sensor array designed to obtain bidimensional mappings of the ion current density profile generated by miniaturized ion thrusters. The objective of this project was the design of an inexpensive tool for fast and basic plume diagnostics of these low-power devices, aiding in the identification of possible sources of losses, lifetime limiting mechanisms and in the qualification procedure of the thrusters. The system is developed to later be used on the production line of the NPT-30 propulsion system at ThrustMe.

The instrument presented consists on an automated arc that holds a set of electrostatic planar probes and is capable of scanning the plume over an angular range of 180 degrees in front of the thruster exit plane in order to map the spatial distribution of ion current density, containing as well all the necessary subsystems for the movement control and synchronous data acquisition. To equalize the signal level measured by each channel, the sensors areas and spacings has been calculated using a gaussian-like distribution, following the predicted plume profile from previous experiments. Because of the expansion of the plasma sheath happening on simple planar probes, the semi-empirical Sheridan's model has been employed in order to correct the measured data.

For the validation of the system, a set of experiments were conducted using the NPT-30 thruster in 19 different operational modes. From the bidimensional numerical integration of the collected data, it was possible to observe that the ion current measured held a close relation to the expected values, suggesting a validation to a certain extent of the proposed technique. The results on the divergence level shown a decreasing trend with the perveance value, suggesting that the thruster operation can be further optimized concerning the beam divergence, with following increase of the angular efficiency by few percent.

With the satisfactory results collected during this work, the further development of the sensor array will be conducted in order to decrease the measurement errors, improve its automation, and ultimately transform it in an industrial validation tool for the electric propulsion systems produced by ThrustMe. The foreseen improvements of the instrument include modifications to the probes for the inclusion of guard-rings and filtering devices, implementation of high precision measurement system for angular position, and the automatic generation of measurement reports.

VI. Acknowledgments

This work was partly funded by the European Commission's Horizon 2020 research and innovation program under grant agreement No. 823337. The authors would like to thank and acknowledge the important contributions given by Antoine Poyet, Florian Marmuse and Sri Harsha Pavuluri.

VII. Bibliography

- [1] I. Levchenko, K. Bazaka, Y. Ding, Y. Raitses, S. Mazouffre, T. Henning, P. Klar, S. Shinohara, J. Schein, L. Garrigues, M. Kim, D. Lev, F. Taccogna, R. Boswell, C. Charles, H. Koizumi, Y. Shen, C. Scharlemann, M. Keidar and S. Xu, "Space micropropulsion systems for Cubesats and small satellites: From proximate targets to furthestmost frontiers," *Applied Physics Reviews*, vol. 1, p. 011104, March 2018.
- [2] A. D. Ketsdever and M. M. Micci, *Micropropulsion for Small Spacecraft*, AIAA, 2012.
- [3] R. E. Wirz, "Miniature Ion Thrusters: A Review of Modern Technologies and Mission Capabilities," *34th International Electric Propulsion Conference*, 2015.
- [4] I. H. Hutchinson, *Principles of Plasma Diagnostics*, Cambridge University Press, 2009.
- [5] S. Mazouffre, G. Largeau, L. Garrigues, C. Boniface and K. Dannenmayer, "Evaluation of various probe designs for measuring the on current density in a Hall thruster plume," in *35th International Electric Propulsion Conference*, Atlanta, 2017.
- [6] D. Lee and N. Hershkowitz, "Ion collection by planar Langmuir probes: Sheridan's model and its verification," *Physics of Plasmas*, vol. 14, no. 14, p. 033507, 2007.
- [7] J. Rovey, M. Walker, A. Gallimore and P. Patterson, "Magnetically filtered Faraday probe for measuring the ion current density profile of a Hall thruster," *Review of Scientific Instruments*, vol. 77, no. 1, p. 013503, 2006.
- [8] D. Brown, M. Walker, J. Szabo, W. Huang and J. Foster, "Recommended Practice for Use of Faraday Probes in Electric Propulsion Testing," *Journal of Propulsion and Power*, vol. 3, pp. 582-613, May 2017.
- [9] R. R. Hofer, M. L. R. Walker and A. D. Gallimore, "A Comparison of Nude and Collimated Faraday Probes for Use with Hall Thrusters," in *27th International Electric Propulsion Conference*, Pasadena, 2001.
- [10] C. C. Farnell, M. M. Schmidt, R. L. Millot, D. J. Warner, K. Siler-Evans and J. D. Williams, "Multi-Axis Plasma Profiling System for Characterization of Plasma Thruster Plumes," in *42nd AIAA/ASME/SAE/ASEE Joint Propulsion Conference & Exhibit*, Sacramento, 2006.
- [11] A. Szelecka, M. J. and J. Kurzyna, "Plasma beam structure diagnostics in krypton," *Laser and Particle Beams*, vol. 36, no. 2, pp. 219-225, 2018.
- [12] A. Neumann, "Update on diagnostics for DLR's Electric Propulsion Test Facility," in *6th Russian-German Conference on Electric Propulsion and Their Application*, Samara, 2017.
- [13] D. Rafalskyi and A. Aanesland, "Brief review on plasma propulsion with neutralizer-free systems," *Plasma Sources Science and Technology*, vol. 25, no. 4, p. 043001, 2016.
- [14] T. Lafleur and D. Rafalskyi, "Radio-frequency biasing of ion acceleration grids," *Plasma Sources Science and Technology*, vol. 27, no. 12, p. 125004, 2018.
- [15] D. Rafalskyi and A. Aanesland, "Plasma acceleration using a radio frequency self-bias effect," *Physics of Plasmas*, vol. 22, no. 6, p. 063502, 2015.
- [16] D. Rafalskyi and A. Aanesland, "A Neutralizer-Free Gridded Ion Thruster Embedded Into a 1U Cubesat Module," in *35th International Electric Propulsion Conference*, Atlanta, 2017.
- [17] M. Marino, F. Cichocki and E. Ahedo, "A collisionless plasma thruster plume expansion model," *Plasma Sources Science and Technology*, vol. 24, no. 3, p. 035006, 2015.
- [18] T. E. Sheridan, "How big is a small Langmuir probe?," *Physics of Plasmas*, vol. 7, no. 7, pp. 3084-3088, 2000.
- [19] G. Aston, H. Kaufman and P. Wilbur, "Ion beam divergence characteristics of two-grid accelerator systems," *AIAA Journal*, vol. 16, no. 5, pp. 516-524, 1978.